European Scientific Journal June 2015 edition vol.11, No.18 ISSN: 1857 – 7881 (Print) e - ISSN 1857- 7431

ADSORPTIVE REMOVAL OF DYES FROM SYNTHETIC WASTEWATER USING ACTIVATED CARBON FROM TAMARIND SEED

Okoli, C. A.
Onukwuli, O.D.
Okey-Onyesolu
C. F., Okoye, C. C
Department of Chemical Engineering,
Nnamdi Azikiwe University, Awka, Nigeria

Abstract

Activated carbon prepared from seed (*Tamarindus indica)* was utilized for the removal of orange G and safranin O dyes from aqueous solution. Chemical activation using orthophosphoric acid (H_3PO_4) was employed for the preparation of activated carbon. The effect of various factors namely; particle size, pH, adsorbent dosage, ion concentration, and contact time was studied to identify the adsorption capacity of the tamarind seed. The percentage of dye adsorbed was found to be dependent on these factors. The Langmuir, Freundlich, and Temkin isotherm models are fitted into the graphs, but the Freundlich isotherm model is best-fitted into the experimental data. The pseudo-first order, pseudo-second order, Elovich, and Bhattacharya-Venkobachor kinetic models were also fitted into the graphs, but pseudo-second order is best fitted into the experimental data. The thermodynamic parameters such as enthalpy, entropy, and free energy were evaluated using the Van't Hoff equations. The negative free energy (ΔG) and negative enthalpy (ΔH) indicate the feasibility and exothermic nature of the adsorption process. The positive entropy (ΔS) shows the increased randomness of the solid/solution interface during the adsorption process. The chemical functional groups, crystalline nature, and the surface morphology of the carbon adsorbents were studied by Fourier Transform Infrared (FTIR) spectroscopy, X-ray Diffraction (XRD) and Scanning Electron Microscopy (SEM). Characteristics of the activated carbons were determined using standard methods.

Keywords: Adsorption, dyes, tamarind seed, isotherms, kinetics, thermodynamics

Introduction

Environmental pollution control has been an issue of major concern in many countries. However, air pollution and water pollution constitutes the major environmental pollution in several countries. Consequently, open burning leads to air pollution, while industrial effluent and domestic sewage leads to water pollution. Water pollution results to bad effects on public water supplies which can cause health problem, while air pollution can cause lung diseases, burning eyes, cough, and chest tightness. The environmental issues surrounding the presence of colour in effluent is a continuous problem for dye stuff manufacturers, dyers, finishers, and water companies (Kesari *et al.*, 2011). The contaminants such as dyes, heavy metal, cyanide, toxic organics, nitrogen, phosphorus, phenols, suspended solids, colour, and turbidity from industries and untreated sewage sludge from domestics, are becoming of great concern to the environmental and public health. Therefore, the treatment of these pollutions is very important (Cheremisinoff, 1993).

Dye is a natural or synthetic colouring material, whether soluble or insoluble which impact its colour to a material by staining or being imbibed by it, and which is employed from a solution of fine dispersion, sometimes with the aid of mordant. They are widely used in textile, paper, leather, and mineral processing industries to colour their product. Their presence in wastewater causes adverse effects in human and aquatic life when disposed into the environment (Wang *et al*., 2004). Many types of dye used in textile industries are direct, reactive, acid, and basic dyes. However, these dyes are invariably left in the industrial wastes. This is because they have synthetic origin and complex aromatic molecular structures, which makes them inert and difficult to biodegrade when discharged into waste streams. Also, people overlook their undesirable nature. Some dyes and their degradation products may be carcinogens and toxins, which are important sources of water pollution. Thus, their treatment becomes a major problem to environmental managers. Some dyes are harmful to aquatic life in rivers where they are discharged, because they can reduce light penetration into water, decrease the efficiency of photosynthesis in aquatic plant, and have adverse effect on their growth (Gurses *et al*., 2004). Furthermore, dyes can also cause severe damage to human beings such as the malfunction of kidney, reproductive system, liver, brain, and the central nervous system (Andre et al., 2011). The occupational exposure of workers in the textile industry is linked to a higher bladder cancer risk. Hence, the removal of dye has become an important aspect of wastewater treatment in industries. Various processes like adsorption, coagulation, flocculation, biosorption, photo-decomposition, ultra-filtration, oxidizing

agents, membrane, and electrochemical processes have been used in the treatment of wastewater (Ho and Chiang, 2001).

Adsorption process is a process by which a gas, liquid or solid adheres to the surface of a solid, but does not penetrate it (Klaus Christmann, 2010). The adsorbing phase is the adsorbent, while the material concentrated or adsorbed at the surface of the phase is the adsorbate. Adsorption process has been found to be an efficient and economic process to remove dyes, pigments, and other colourants (Wang *et al*., 2004). In addition, it has been found to be superior to other techniques of wastewater treatment in terms of cost, simplicity of design, ease of operation, and insensitivity to toxic substances (Garg *et al*., 2004). Adsorbents such as activated carbon, peat, chitin, clay, and others can be used. Adsorption using activated carbon is rapidly becoming a prominent method of treating aqueous effluents and has been used in the industrial processes for variety of separation and purification techniques.

Furthermore, activated carbon is used as adsorbent for dye removal from wastewater. This could be related to their extended surface area, high adsorption capacity, microporous structure, and special surface reactivity. Therefore, the removal of dyes through activated carbon adsorption is very effective. At present, there is a growing interest in using other low cost sorbents for dye removal. Many lignocellulosic materials including coir pith, sunflower stalks, corncob and barley husk, rice husk, and other materials have been used as a low cost dye sorbents (Banat *et al*., 2003).

The purpose of this work is to test the effectiveness of activated carbon produced from tamarind seed for the removal of Orange G and Safranine O dyes from synthetic wastewater by adsorption technique.

Experimental Method

Adsorbent and Adsorbates

Tamarind seeds were obtained from Mallam Nuhu farm in Kano state. The seeds were washed thoroughly with de-ionized water to remove unwanted materials. They were dried in an air-drying oven at 110^{o}C for 24hours. However, the dried sample was carbonized in a muffle-furnace at 500^{o}C for 1hour. The sample was impregnated with 60% weight of orthophosphoric acid at the ratio of 1:2(wt %). Then, the resulting carbons were washed with de-ionized water until the leachate was between a pH of 6-7. They were then dried in an air-drying oven at 110^{o}C for 6hours. Also, the sample was crushed and was made to pass through different sieve sizes. Finally, the sample was stored in a tight bottle ready for use.

All dyes were obtained from Onitsha market in Anambra state. The pH solution was adjusted by adding a small amount of 0.1M HCl or NaOH.

Characterization of Activated Carbon

The ash content was determined using ASTM E1755-01 (ASTM, 2003). The pH of the carbon was determined using standard test ASTM D 3838-80 (ASTM, 1996). Moisture content of activated carbon was determined using standard test ASTM D 2867-91 (ASTM, 1991). The specific surface area of the activated carbon was estimated using Sear's method (Gregg and Sing, 1982). In addition, the iodine number was determined based on ASTM D 4607-86 (1986) using the sodium thiosulphate volumetric method.

Batch Adsorption Studies

Batch adsorption equilibrium experiments were conducted for the adsorption of orange G dye ($C_{16}H_{10}N_2Na_2O_7S_2$) and safranin O dye ($C_{20}H_{19}ClN_4$) on activated carbon of tamarind seed as a function of particle size, initial pH, adsorbent dosage, ion concentration, and contact time. This was done by adding 0.5g of adsorbent to 100ml of adsorbate solution of concentration (100mg/L) having a known pH in a conical flask and mixed on a Wincom magnetic stirrer (hot plate SH85-2) at 30^{o}C for 60mins. Based on the effect of the particle size, 0.5g of adsorbent with different adsorbent particles passing through 75µm sieve mesh size and retained in 1000µm was added to different conical flasks. These flasks contain 100ml of adsorbate solution of concentration (100mg/L) which was mixed for 60mins. Based on the effect of the pH, dye solution was measured into different conical flask and adjusted in the pH range of 2, 4, 6, 8, and10 with dilute HCl (0.1M) and NaOH (0.1M) solutions through the use of a pH meter. Based on the effect of adsorbent dosage, different adsorbent dose of 0.3, 0.5, 1, 1.5, and 2g was added in each conical flask containing 100ml of adsorbate solution of concentration (100mg/L), and was stirred for 60mins. Based on the effect of ion concentration, 0.5g of adsorbent was added to each conical flask containing 100ml of adsorbate solutions of different concentrations of 50, 100, 150, 300, and 500mg/L which was stirred for 60mins. Based on the effect of contact time, 0.5g of adsorbent was added to 100ml of adsorbate solution of concentration (100mg/L) and was stirred at different time intervals of 3, 5, 10, 20, 30, 45, 60, 90, 120, and 150mins. Furthermore, the solution was withdrawn from the reaction mixture at a fixed time interval, and was filtered using Whatman no.1 filter paper. The amount of unadsorbed dye in the supernatant solutions was measured with the aid of a Wincom visible spectrophotometer at wavelengths of 480nm for orange G dye and 510nm for safranin O dye.

Therefore, the amount of adsorption at equilibrium (q_e) (mg/g) and the percentage adsorption (%) were computed as follows:

$$q_e = [(C_o - C_e)\,{}^{V}/_{M}] \quad (1)$$

$$\%\ adsorbed = \left[{}^{(C_o - C_e)}/_{C_o}\right] x\ 100 \quad (2)$$

Where; C_o and C_e are the initial and final dye concentration respectively (mg/L) at any time (t).

V is the volume of the solution (L) and M is the mass of the adsorbent used (g).

Results and Discussion

Characteristics of Activated Carbon Derived from Tamarind Seed.

The physico-chemical characteristics of activated carbon are shown in Table 1. The higher surface area (983m^2/g) may be due to the restricted pore shrinkage during activation indicating high porosity. The typical range of values for commercial activation according to Haimour and Emeish (2006) is 600-1500m^2/g. Thus, the low ash content value (2.35%) indicates that the activated carbons have low inorganic content and high fixed carbon. This is because ash content can reduce the efficiency of reactivation. Therefore, the lower the ash content, the better the activated carbon. Moisture content dilutes the carbon and increases the weight during treatment process. Thus, the lower the moisture contents in activated carbons, the better. The moisture content (3.00%) was found to be low, indicating that the carbon structure has extensive porosity through the activation process. The moisture content value can be compared with the value reported by Verla *et al*. (2012). As reported by Okiemmen *et al*. (2008), the pH of carbon is acceptable in the range of 6 - 8. The pH value of the activated carbon was 6.8. Bulk density is an important variable that must be considered in the design of adsorption column because it can affect the overall cost of the process. Hence, it determines the mass of carbon which can be contained in a filter by a given solids capacity. It also determines the amount of treated liquid that can be retained by the filter cake. However, it can be seen that the bulk density (0.51 g/cm^3) will filter high liquor volume before the available cake space is filled. Iodine number can be obtained by the adsorption of iodine from solution by the activated carbons. It is a measure of the micropore content of the activated carbon, because micropores are created during activation process and are responsible for the large surface area of activated carbons. In addition, the iodine value (865mg/g) shows high micropore content in the activated carbon.

Table 1: Physico-Chemical Characteristics of Activated Carbon Derived from Tamarind Seed

Properties	**Values**
Surface area (m^2/g)	983
Moisture content (%)	3.00
Ash content (%)	2.35
pH	6.80
Bulk density (g/cm^3)	0.51
Iodine number (mg/g)	865

Fourier Transform Infrared Spectroscopy Analysis.

Fourier Transform Infrared Spectroscopy (FTIR) study was carried out to identity the functional groups present in the adsorbents ranging from $600cm^{-1}$ to $4000cm^{-1}$. The adsorption capacity of adsorbent depends upon the porosity as well as the chemical reactivity of the functional groups at the adsorbent surface (Suresh, 2013). The plot of functional groups and their peaks on the carbon adsorbent and acid impregnated carbon adsorbent are shown in Figures 1 and 2. Furthermore, the results presented in Tables 2 and 3 show the presence of alkanes (C-H stretch), alkenes (=C-H stretch), alkynes (-C≡C-), carboxylic acids (O-H bend), aromatics amines (C-N), nitrites (C≡N stretch), aromatics (C-H stretch), alkyl halides, etc. The shift in the wave number of dominant peak associated with the plots showed various surface functional groups. The presence of hydroxyl groups, carbonyl groups, ethers, and aromatic compounds is an evidence of the lignocellulosic structure of tamarind seed which was also observed in other materials such as coconut shell (Andre et al., 2011) and cotton stalks (El-Hendawy et al., 2008).

Table 2: Fourier Transform Infrared Spectrum for Acid Activated Carbon Tamarind Seed

Functional Group	Absorption Peak (cm^{-1})
C-Cl stretch alkyl halides	778.7686
C-H, aromatics	894.0875
C-N stretch aromatic amines	1104.074
C-N stretch aromatic amines	1287.1
N=O bend nitro compounds	1.381.824
C-C stretch (in ring) aromatics	1452.822
-C=C- stretch alkenes	1627.21
-C≡C- stretch alkynes	2176.194
Hydrogen-bonded O-H stretch carboxylic acid	2424.58
Hydrogen-bonded O-H stretch carboxylic acid	2621.008
Hydrogen-bonded O-H stretch carboxylic acid	2706.048
H-C-H stretch alkanes	2850.872
H-C-H stretch alkanes	2989.518
C=C-H stretch alkenes	3091.54
O-H stretch, carboxylic acid	3216.43
N-H stretch in amines, amides	3302.668

O-H stretch, H-bonded, phenols and alcohol	3429.882
O-H stretch, H-bonded, phenols and alcohol	3491.908
O-H stretch in phenols and alcohol	3679.638
O-H stretch in phenols and alcohol	3791.593
O-H stretch in phenols and alcohol	3899.307

Table 3: Fourier Transform Infrared Spectrum for Carbon Tamarind Seed

Functional Group	Absorption Peak (cm^{-1})
-C-H bending R-CH=CH_2	909.1885
C-O stretch, alcohol, carboxylic acid, esters, ethers	1048.632
C-O stretch, alcohol, carboxylic acid, esters, ethers	1142.67
C-N stretch aromatic amines	1313.454
C-H stretch alkanes	1406.053
-C=C- stretch aromatics	1564.395
-C=C- stretch alkenes	1638.292
-C≡C-H stretch alkynes	2187.355
-O-H stretch carboxylic acid	2545.098
-O-H stretch carboxylic acid	2662.83
C-H stretch off C=O	2841.17
O-H stretch carboxylic acid	2964.175
-O-H stretch carboxylic acid	3143.41
N-H stretch 1^o, 2^o amines, amides	3335.602
Hydrogen-bonded O-H stretch phenols and alcohol	3528.681
O-H stretch, free hydroxyl, alcohol and phenols	3628.434
O-H stretch in phenols and alcohols	3828.511

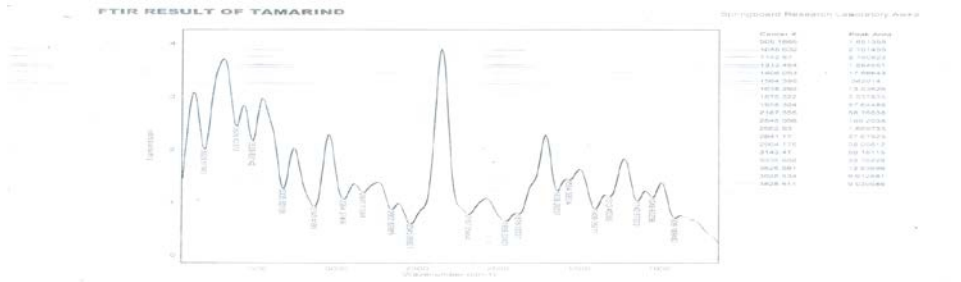

Fig 1: FTIR Spectrum for Carbon Tamarind Seed

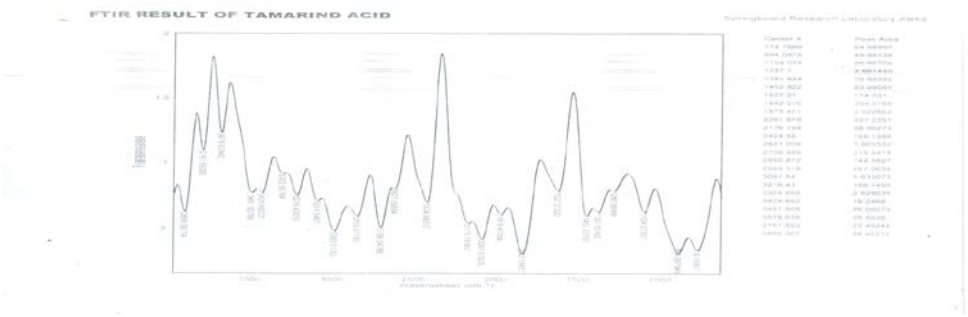

Fig 2: FTIR Spectrum for Acid Activated Carbon Tamarind Seed

X-ray Diffraction Analysis

X-ray diffraction measurement was used to determine the crystal structure of the adsorbents. The XRD patterns for acid activated tamarind seed carbon and activated tamarind seed carbon were demonstrated in Figures 3 and 4 respectively. Higher peaks and broadness were observed in acid activated samples than the non-acid activated samples. Also, the presence of high diffraction peaks and broadness are evidence of good crystallinity of the prepared powdered samples. The intensities for each samples as presented in Figures 3 and 4 are in the range of 10-79^{o}= 2Ɵ. Thus, this indicates that other low intensity peaks corresponding to other crystalline phases of carbon have also been observed.

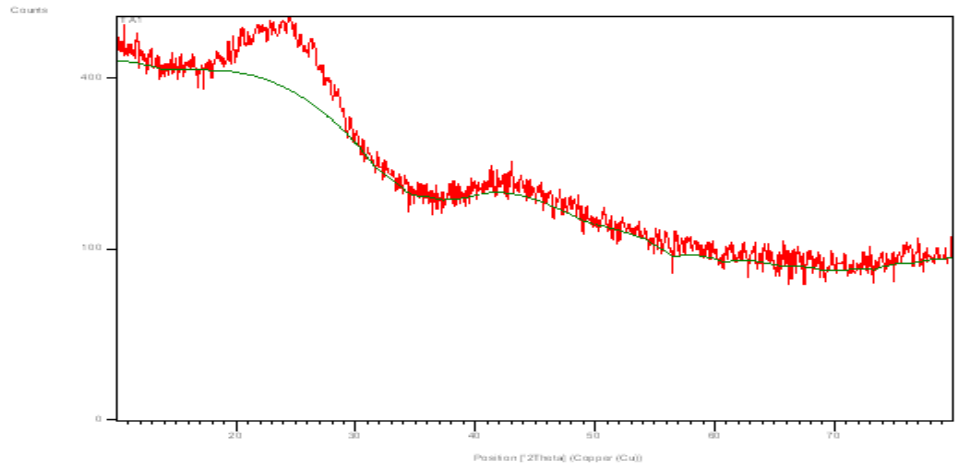

Fig 3: XRD Measurement for Acid Activated Carbon Tamarind

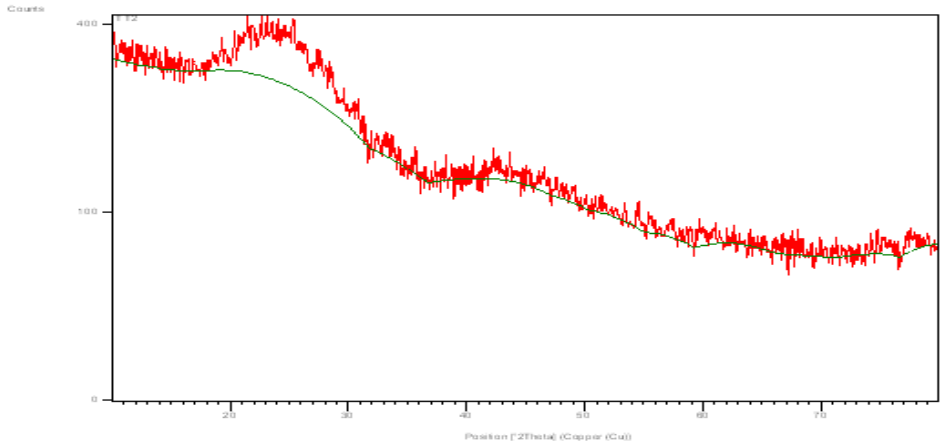

Fig 4: XRD Measurement for Carbon Tamarind Seed

Scanning Electron Micrograph Analysis

Scanning electron micrographs of activated tamarind seed carbon and acid activated tamarind seed carbon are shown in figures 5 to 8. In this work, combinations of lower and higher magnifications were used. These included magnifications of 4000X and 8000X for both samples with 15kV accelerating voltage. In the SEM image at magnification of 4000x (corresponding to specimen area of 20μm^2) for both samples, the micrograph displayed an irregular shape pitted canal-like structure with larger pore size. However, this was observed in the acid activated carbon than in the non-acid activated carbon. At a magnification of 8000x (corresponding to specimen area of 10μm^2), the micrograph for the non-acid activated carbon displayed a larger canal-like structure than those of the 4000X magnification, while the acid activated carbon displayed a net-like structure with larger pore size observed than those of 4000X.

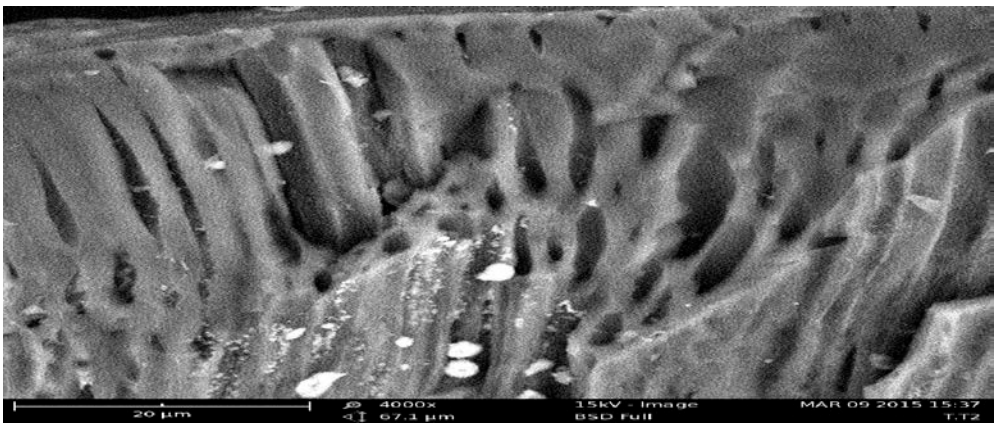

Fig 5: Scanning Micrograph for Activated Tamarind Seed Carbon at 4000X Magnification

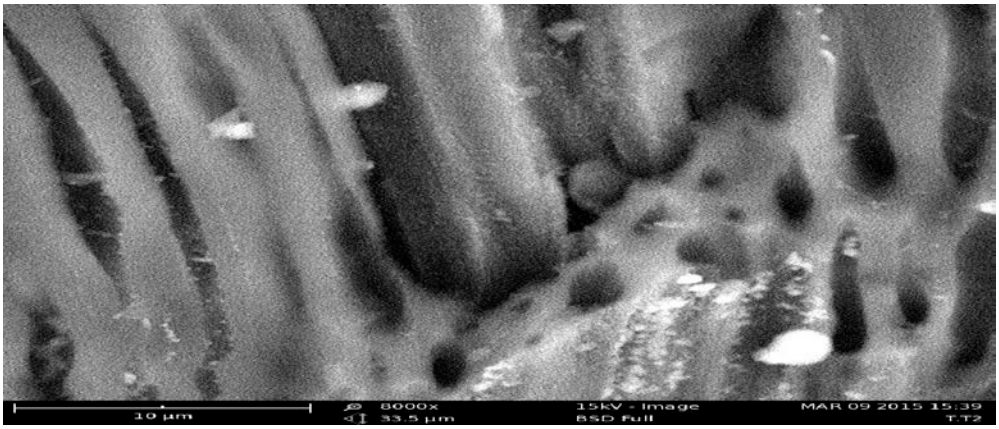

Fig 6: Scanning Micrograph for Activated Tamarind Seed Carbon at 8000X Magnification

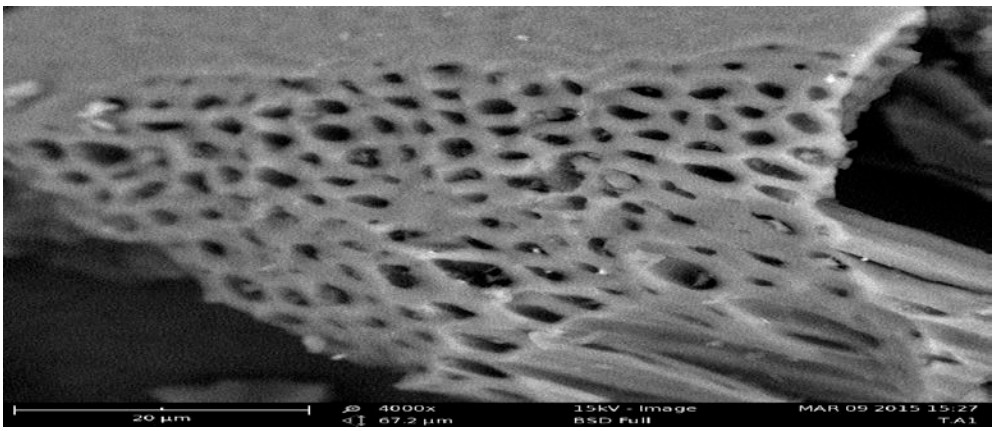

Fig 7: Scanning Micrograph for Acid Activated Tamarind Seed carbon at 4000X Magnification

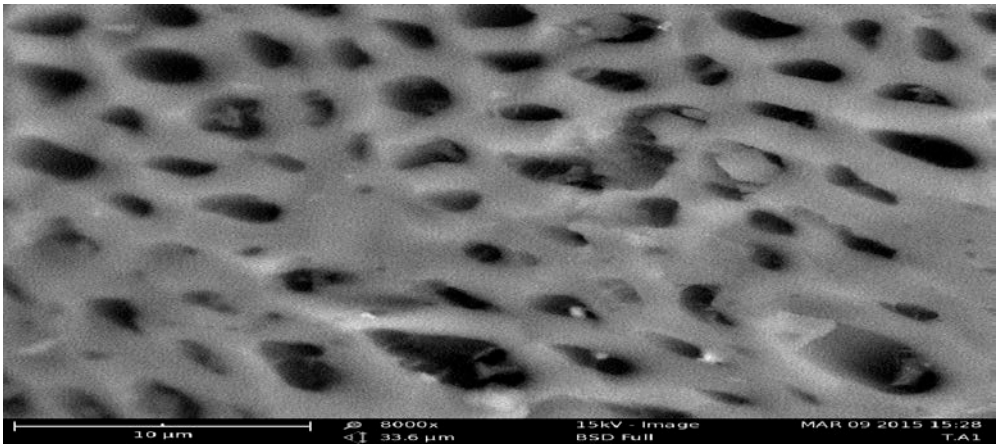

Fig 8: Scanning Micrograph for Acid Activated Tamarind Seed carbon at 8000X Magnification

Effect of Particle Size on the Adsorption Process

The removal of orange G and safranin O dyes using activated carbon of different particle sizes showed that the removal rate decreases with increase in particle size (Figures 15 and 16). The particle sizes ranging from 75µm to 1000µm have percentages of dye adsorbed between the ranges of 68.26% to 19.27% for orange G dye and 87.13% to 34.03% for safranin O dye respectively. This shows that 75µm was the best particle size to be used, because it adsorbed the highest percentage of dye. The relatively higher adsorption with smaller adsorbent particle size may be attributed to the fact that smaller particle yields larger surface area. Thus this provides a greater number of sites for adsorption and implies opening of more micropores. However, similar results were obtained by Rahman *et al*. (2012).

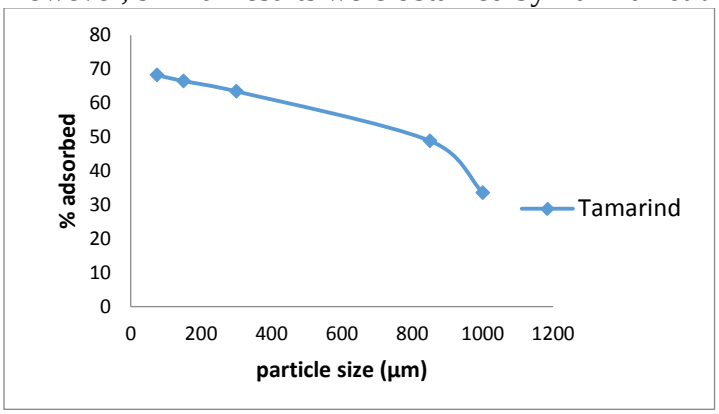

Fig 15: Effect of particle size on acid activated tamarind seed carbon using orange G dye.

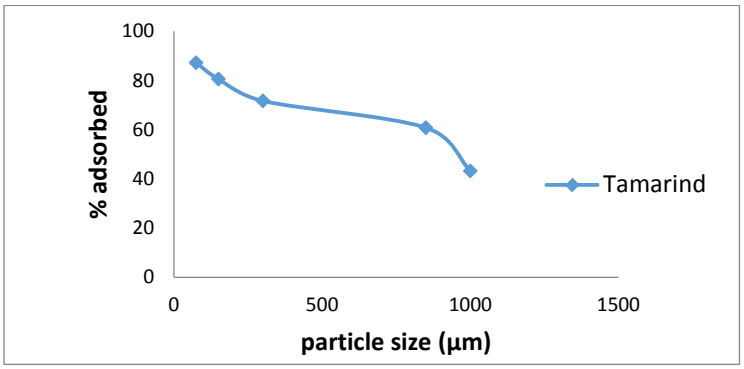

Fig 16: Effect of particle size on acid activated tamarind seed carbon using safranin O dye.

Effect of pH on the Adsorption Process

pH is an important parameter in adsorption study because it controls the degree of ionization and speciation of the adsorbate. The effect of pH on the adsorption of dye into acid activated tamarind seed carbon was studied between the ranges of 2-10. The percentages of dye adsorbed were between the range of 88.08% to 42.97% for orange G dye and 35.00% to 95.52% for safranin O dye. The result showed that the amount of dye adsorbed decreased with increase in the pH value for orange G dye (Figure 17) and increased with increase in pH value for safranin O dye as shown in (Figure 18). This indicates that a low pH was favourable for the adsorption of orange G dye by the adsorbent, because they are anionic dye (acid dye). This is due to the fact that as the pH of the system decreased, the number of negatively charged adsorbent sites decreased also, while the number of positively charged surface sites increased. These effects favoured the adsorption of the negatively charged dye anions due to electrostatic attraction. The high pH favourable for the adsorption of safranin O dye (cationic dye known as basic dye) is due to the fact that as the pH of the system increased, the number of negatively charged adsorbent sites increased also, and the number of positively charged surface sites decreased. This effect favours the adsorption of the positively charged dye cations due to electrostatic attraction. However, similar results were obtained by singh *et al*. (2011).

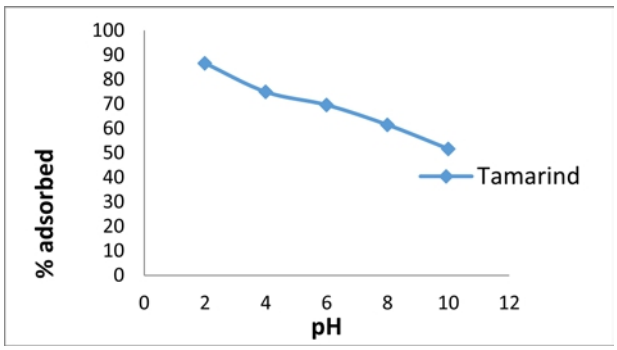

Fig 17: Effect of pH on acid activated tamarind seed carbon using orange G dye.

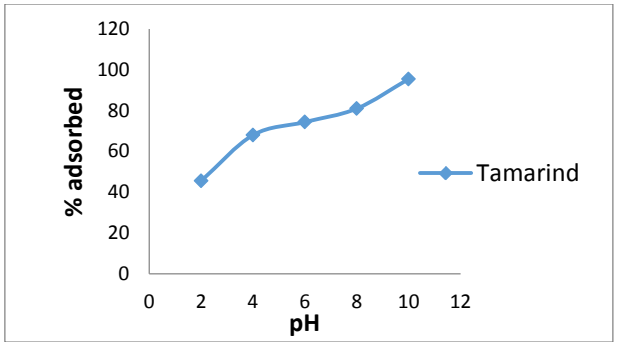

Fig 18: Effect of pH on acid activated tamarind seed carbon using safranin O dye.

Effect of Adsorbent Dosage on the Adsorption Process

Adsorption dosage determines the capacity of an adsorbent for a given initial concentration of the adsorbate (Joseph and Philomena, 2011). The result showed that as the adsorbent dosage increased, the percentage of dye adsorbed increased alsofrom 0.5g to 2g. The percentage of adsorption increased up to 1.0g of adsorbent after which no significant changes in the percentages of dye was adsorbed with an increasing amount of the adsorbent (Figures19 and 20). However, it showed that most of the adsorbents studied attained equilibrium around 1.0g of dosage. The adsorption efficiency increased due to the increased number of adsorption sites and surface area. However, similar results were obtained by Bulut and Aydin (2005).

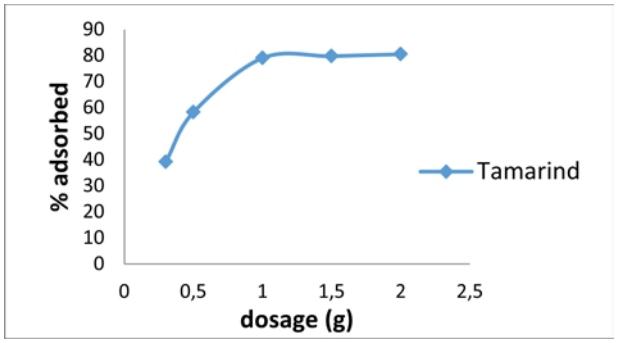

Fig 19: Effect of dosage on acid activated tamarind seed carbon using orange G dye.

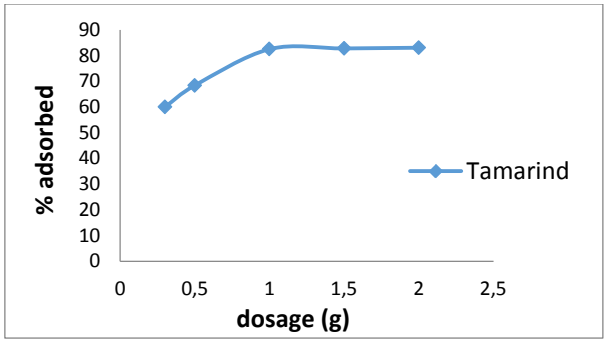

Fig 20: Effect of dosage on acid activated tamarind seed carbon using safranin O dye.

Effect of Initial Concentration on the Adsorption Process

The initial concentration of adsorbate plays an important role, as a given mass of adsorbent can adsorb only a certain amount of a solute. The concentrations ranged from 50mg/L to 500mg/L. As presented in Figures 21 and 22, the result showed that the more the concentration of the solution, the smaller the percentage of dye that a given mass of adsorbent can adsorb. In a low concentration range, the fractional adsorption is higher compared to the high concentration range. This is due to the fact that at a lower concentration, the available sites for adsorption become more, while at a higher concentration, the available sites become fewer. Thus, the percentage of dye removal was dependent upon the initial concentration. However, similar results were obtained by Khan *et al*. (2009) and Ozacar *et al*. (2003).

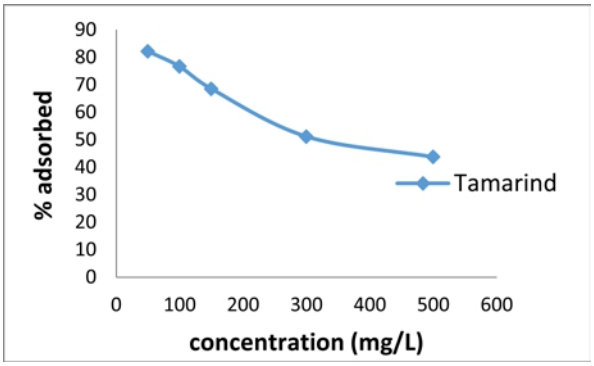

Fig 21: Effect of concentration on acid activated tamarind seed carbon using orange G dye.

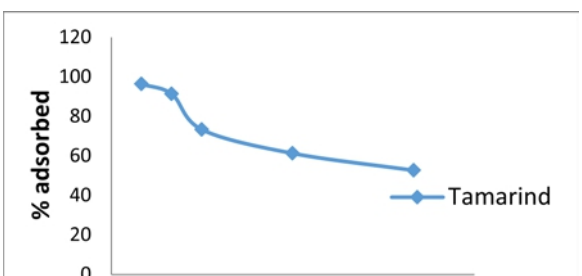

Fig 22: Effect of concentration on acid activated tamarind seed carbon using safranin O dye.

Effect of Contact Time on the Adsorption Process

The contact time was found to play significant roles in the process of dye removal from wastewater by adsorption at a particular temperature, pH, adsorbent dosage, and particle size. The batch equilibrium adsorption time of orange G, and safranin O dyes on acid activated tamarind seed were investigated at different times (3, 5, 10, 20, 30, 45, 60, 90, 120, and 150mins). As shown in Figures 23 and 24, the rapid uptake of the dyes species and the establishment of equilibrium within a short period indicated the efficiency of the adsorbent for its use in wastewater treatment. It can be seen that the removal of the dyes reaches maximum at 60mins for orange G and 45mins for safranin O dye and becomes gradual thereafter. This indicates that the rate of adsorption is very fast; and after that, no significant change in the extent of adsorption was observed (Singh *et al*., 2011).

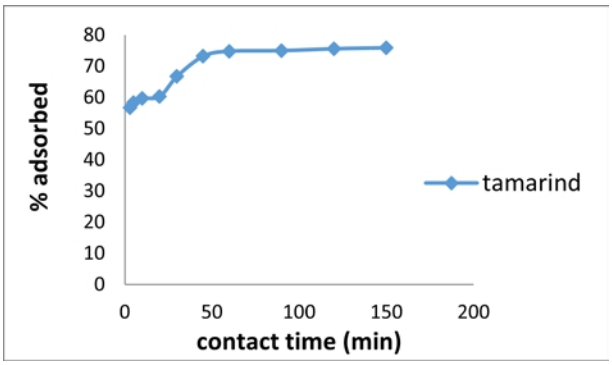

Fig 23: Effect of contact time on acid activated tamarind seed carbon using orange G dye

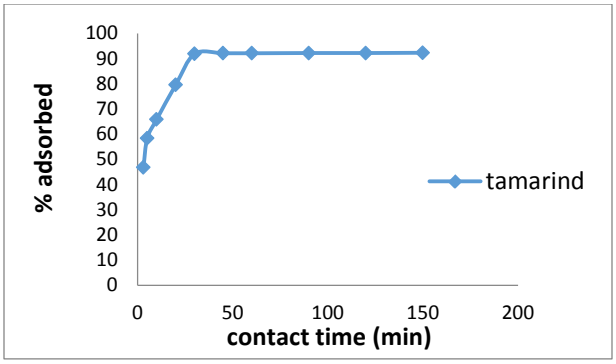

Fig 24: Effect of contact time on acid activated tamarind seed carbon using safranin O dye

Langmuir Isotherm Model

The Langmuir isotherm model is given by:

$$q_e = {}^{Q_o b C_e}/_{1 + \mathrm{bC_e}} \qquad (3)$$

The linearized form of the Langmuir equation can be written in the form (Sekar *et al.*, 2004):

$${}^{C_e}/_{q_e} = {}^{1}/_{Q_o} C_e + {}^{1}/_{Q_o} b \qquad (4)$$

Where q_e is the amount of adsorbate per unit mass of adsorbent (mg/g); C_e is the equilibrium concentration of adsorbate (mg/L); and the Langmuir constants b and Q_o represents the adsorption equilibrium constant and the maximum adsorption capacity, respectively. A straight line graph with slope of $1/Q_o$ and intercept b was obtained when C_e/q_e was plotted against C_e. Therefore, this indicates that the adsorption follows the Langmuir isotherm as shown in figures 25 and 26.

The study of equilibrium parameter R_L, which is a dimensionless constant and is referred to as separation factor is given by:

$$R_L = {}^{1}/_{1 + (1 + \mathrm{bC_o})} \qquad (5)$$

Where; C_o is the initial concentration. The R_L values indicate the adsorption to be favourable if ($0< R_L<1$), unfavourable if ($R_L>1$), linear if ($R_L=1$) or irreversible if ($R_L=0$). The R_L values issued from this study were ranged from 0.276 to 0.301 for orange G dye and 0.225 to 0.303 for safranin O dye, while the correlation coefficients (R^2) ranged from 0.967 to 0.970 for orange G dye and 0.904 to 0.927 for safranin O dye with the increase in temperature from 303K to 323K, respectively (Tables 4 and 5). These results have indicated that the description of adsorption process by means of

Langmuir isotherm model is favourable and also fits into the graph. However, similar results were obtained by Juang *et al*. (1997).

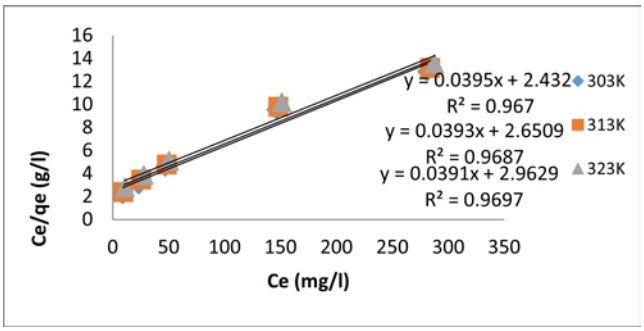

Fig 25: Langmuir isotherm plot for orange G dye on acid activated tamarind seed carbon.

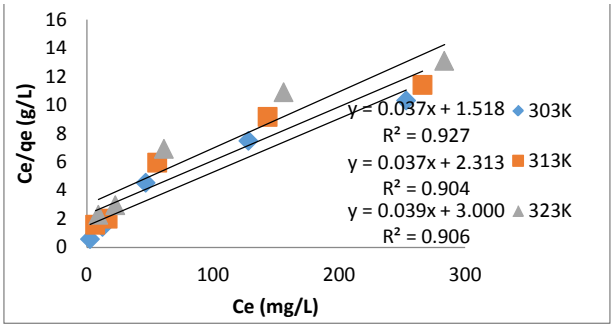

Fig 26: Langmuir isotherm plot for safranin O dye on acid activated tamarind seed carbon.

Freundlich Isotherm Model

The Freundlich adsorption isotherm (Ozacar, 2003) is given by:

$$q_e = K_f C_e^{1/n} \quad (6)$$

A linear form of the expression above is written as:

$$\log q_e = \log K_f + {}^1/_n \log C_e \quad (7)$$

Where K_f and n are Freundlich constants. K_f and n corresponding respectively to adsorption capacity of adsorbent and adsorption intensity have been obtained from the intercepts and slopes of the linear plot of $\log q_e$ against $\log C_e$ as shown in Figures 27 and 28. The magnitude of adsorption intensity n gives an indication of the favourability of the adsorption process. Ho and Chang, (2001) reported that the favorability of the process is achieved if n lies in the range of 1–10. The adsorption intensity (n) varied from 2.155 to 2.004 for orange G dye and 2.915 to 2.212 for safranin O dye with the increase in temperature from 303K to 323K respectively as shown in Tables 4 and 5. The values of the adsorption intensities obtained are in

conformity with the requirement for physical adsorption process, which characterize it to be favourable.

The correlation coefficients R^2 ranged from 0.986 to 0.989 using orange G dye and 0.943 to 0.963 with safranin O dye (Table 4 and 5). This shows that the adsorption of the dyes on the adsorbent followed Freundlich isotherm. However, similar results were obtained by Ho and Chang (2001).

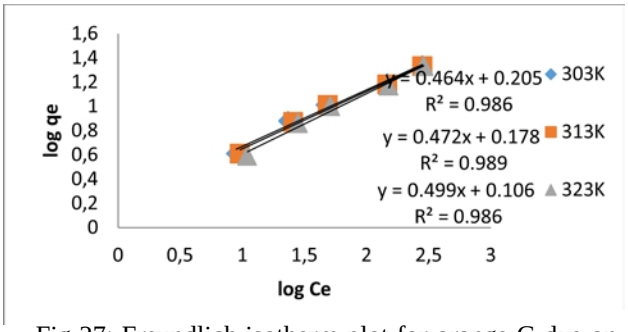

Fig 27: Freundlich isotherm plot for orange G dye on acid activated tamarind seed carbon.

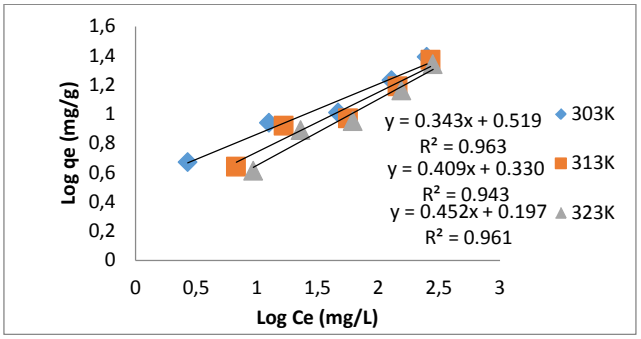

Fig 28: Freundlich isotherm plot for safranin O dye on acid activated tamarind seed carbon.

Temkin Isotherm Model

The Temkin isotherm (Aharoni and Sparks, 1991) is given by:

$$q_e = {}^{RT}/_{b} \ln(A_T\, C_e) \qquad (8)$$

The linear form of Temkin isotherm can be expressed as:

$$q_e = {}^{RT}/_{b_T} \ln A_T + {}^{RT}/_{b_T} \ln C_e \qquad (9)$$

Where A_T is the Temkin isotherm equilibrium binding constant (L/g); b_T is the Temkin isotherm constant; R is the universal gas constant (8.314J/mol/K); T is the temperature at 298K; and C_e is the equilibrium concentration (mg/L). Temkin isotherm constant b_T and Temkin isotherm equilibrium binding constant A_T were obtained from the intercepts and slopes of the linear plot of q_e versus $\ln C_e$ as shown in Figures 29 and 30. The

correlation coefficients R^2 ranged from 0.960 to 0.963 for orange G dye and 0.862 to 0.890 for safranin O dye as the temperature increased from 303K to 323K, respectively, as shown in Tables 4 and 5. This shows that the data for orange G dye conforms more to Temkin isotherm model than safranin O dye. However, similar results were obtained by Dada *et al*. (2012).

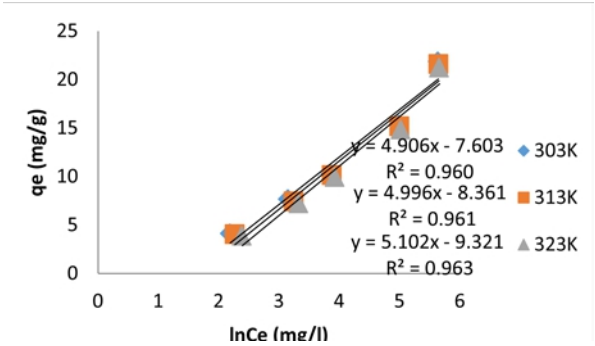

Fig 29: Temkin isotherm plot for orange G dye on acid activated tamarind seed carbon.

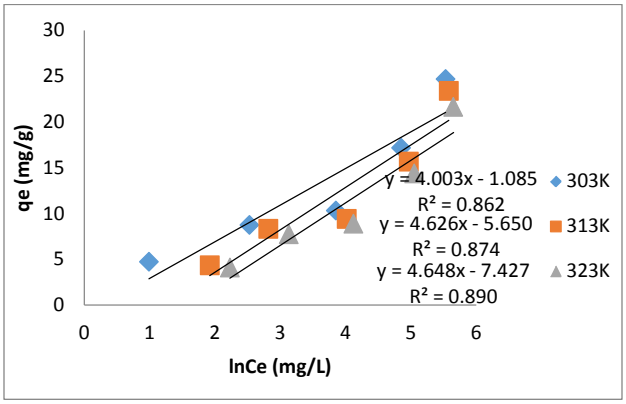

Fig 30: Temkin isotherm plot for safranin O dye on acid activated tamarind seed carbon.

The Dubinin-Radushkevich equation (Hasany and Chaudhary, 1996) is given by:

$$q_e = (q_D)\exp(-B_D\varepsilon^2) \quad (10)$$

The linear form of Dubinin-Radushkevich equation is given by:

$$\ln q_e = \ln q_D - (B_D\varepsilon^2) \quad (11)$$

Where q_D is the theoretical isotherm saturation capacity (mg/g), B_D is the Dubinin-Radushkevich isotherm constant (mol^2/kJ^2), and ε is the Polanyi potential.

$$\varepsilon = RT\ln(1 + {}^{1}/_{C_e}) \quad (12)$$

Where R is the universal gas constant (8.314J/mol/K); T is the temperature at 298K; and C_e is the equilibrium concentration (mg/L). The constant B_D gives the mean free energy E of sorption per molecule of the sorbates when it is transferred to the surface of the solid from infinity in the solution and can be computed using the relationship;

$$E = {}^{1}/_{\sqrt{2B_D}} \qquad (13)$$

The Dubinin-Radushkevich parameters B_D and q_D (theoretical isotherm saturation capacity) were calculated from the slopes and intercepts of the linear plots of $\ln q_e$ versus ε^2 as shown in Figures 31 and 32. The correlation coefficients R^2 using orange G dye ranged from 0.727 to 0.738 and 0.619 to 0.695 for safranine O dye as temperature increased from 303K to 323K (Tables 4 and 5). This shows that the graph did not conform to the Dubinin-Radushkevich isotherm.

The mean free energy E reveals the nature of adsorption. Thus, if the value of adsorption energy E is less than 8KJ/mol, adsorption process is physical; but if it is ranged from 8 to 16KJ/mol, it is a chemical adsorption. The E values obtained ranged from 0.158 to 0.129KJ/mol using orange G dye and 0.500 to 0.224KJ/mol using safranine O dye. The E values obtained are less than 8KJ/mol, indicating that it is a physio-sorption process. However, similar results were obtained by Dada *et al*. (2012).

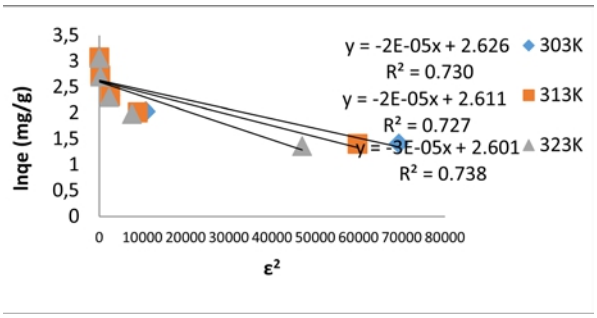

Fig 31: Dubinin-Radushkevich isotherm plot for orange G dye on acid activated tamarind seed carbon.

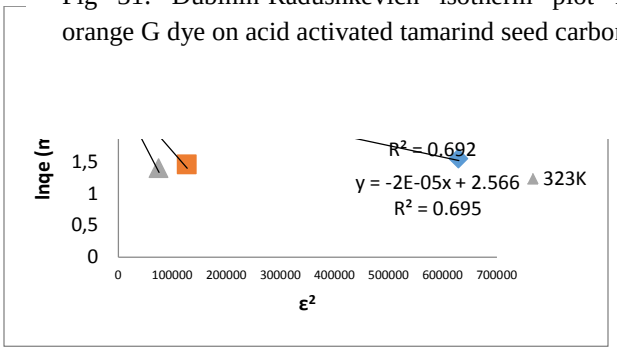

Fig 32: Dubinin-Radushkevich isotherm plot for safranin O dye on acid activated tamarind seed carbon.

Table 4: Adsorption Isotherm Studies Parameters for Acid Activated Tamarind Seed Using Orange G Dye

Models	**Parameters**	**303K**	**313K**	**323K**
Langmuir	Q (mg/g)	25.316	25.445	25.575
	b (L/mg)	0.016	0.015	0.013
	R_L	0.276	0.287	0.301
	R^2	0.967	0.969	0.970
Freundlich	n	2.155	2.119	2.004
	K_f (L/g)	1.603	1.507	1.276
	R^2	0.986	0.989	0.986
Temkin	b_T (J/mg)	505.009	495.911	485.608
	A_T (L/g)	0.212	0.188	0.161
	R^2	0.960	0.961	0.963
Dubinin-Radushkevich	B (mol^2/J^2)	$-2x10^{-5}$	$-2x10^{-5}$	$-3x10^{-5}$
	q_s (mg/g)	13.818	13.613	13.477
	E (KJ/mol)	0.158	0.158	0.129
	R^2	0.730	0.727	0.738

Table 5: Adsorption Isotherm Studies Parameters for Acid Activated Tamarind Seed Using Safranin O Dye

Models	**Parameters**	**303K**	**313K**	**323K**
Langmuir	Q (mg/g)	27.027	27.027	25.641
	b (L/mg)	0.024	0.016	0.013
	R_L	0.225	0.278	0.303
	R^2	0.927	0.904	0.906
Freundlich	n	2.915	2.445	2.212
	k_f	3.304	2.138	1.574
	R^2	0.963	0.943	0.961
Temkin	b_T (J/mg)	618.929	535.575	533.04
	A_T (L/g)	0.763	0.295	0.202
	R^2	0.862	0.874	0.890
Dubinin-Radushkevich	B (mol^2/J^2)	$-2x10^{-6}$	$-1x10^{-5}$	$--2x10^{-5}$
	q_s (mg/g)	14.325	14.041	13.014
	E (KJ/mol)	0.500	0.224	0.158
	R^2	0.619	0.692	0.695

Adsorption Kinetics

Pseudo-First Order Kinetic Model

The pseudo-first order rate expression popularly known as Lagergren equation is generally expressed by this equation (Lagergren 1898):

$$\ln(q_e - q_t) = \ln q_e - K_1 t \qquad (14)$$

Where q_e and q_t are the amount of dye adsorbed at equilibrium time and at any time t, respectively (mg/g); K_1 is the pseudo-first order adsorption rate constant (min^{-1}); and t is the contact time (min). The Pseudo-first order rate constants, K_1 and q_e at different temperatures were determined from the slope and intercept of the plot of $Ln(q_e-q_t)$ versus t as presented in figures 33 and 34 . The results of the q_e and K_1 were evaluated and listed in Tables 6 and 7. The values of the correlation coefficient R^2 ranged from 0.940 to 0.972 for orange G dye and 0.763 to 0.910 for safranin O dye. The values for orange G dye was high showing that Pseudo-first order kinetic model describes the adsorption process, but was not applicable to safranin O dye. However, similar results were obtained by Ho and Mckay (1998).

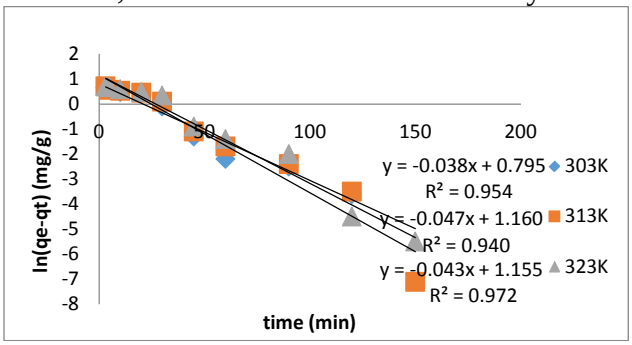

Fig 33: Pseudo-First order kinetics plot for orange G dye on acid activated tamarind seed carbon.

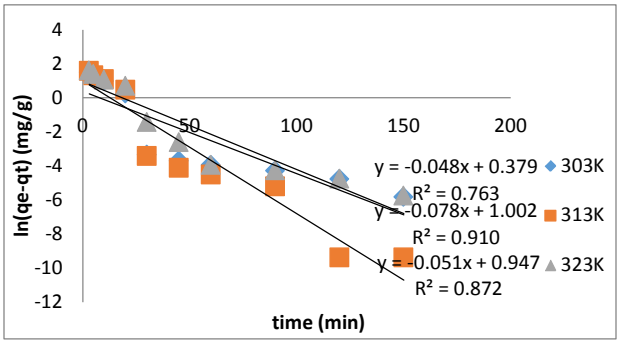

Fig 34: Pseudo-First order kinetics plot for safranin O dye on acid activated tamarind seed carbon.

Pseudo-First Order Kinetic Model

The pseudo-second order equation is expressed as (Ho and Mckay, 1998):

$$dq/dt = K_2(q_e - q_t)^2 \quad (15)$$

The integrated form of the expression gives:

$$t/q_t = 1/K_2q_e + t(1/q_e) \quad (16)$$

Where; K_2 is the pseudo-second adsorption rate constant (g/mgmin). The pseudo-second order rate constants, K_2 and q_e at different temperatures were determined from the slope and intercept of the plot of t/q_t versus t as presented in Figures 35 and 36. The results of K_2 and q_e were evaluated and listed in Tables 6 and 7. The calculated q_e values agree with the experimental q_e values. The correlation coefficient values R^2 was 0.999 for orange G dye and 0.999 for safranin O dye. These results show that the correlation coefficient of pseudo-second order was higher than that of pseudo-first order, which implies that the adsorption system studied follows the pseudo-second order kinetics model better. However, similar results were obtained by Horsfall *et al*. (2004).

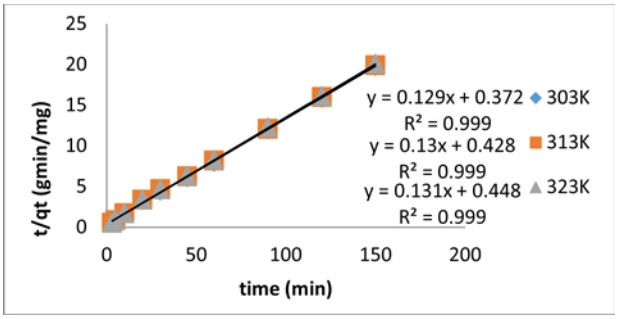

Fig 35: Pseudo-second order kinetic plot for orange G dye on acid activated tamarind seed carbon.

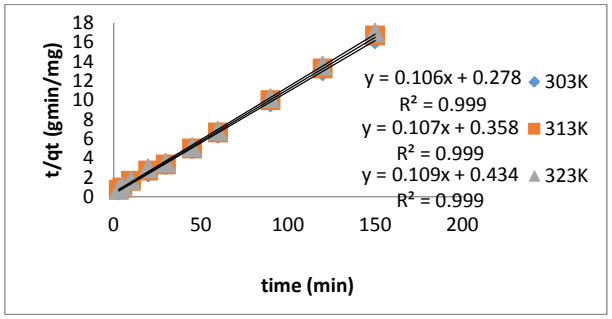

Fig 36: Pseudo-second order kinetic plot for safranin O dye on acid activated tamarind seed carbon.

Elovich Kinetic Model

The Elovich equation is expressed as (Oladoja *et al*., 2008):

$$dq/dt = \alpha_e^{-\beta q_t} \quad (17)$$

Integrating this equation for the boundary conditions gives:

$$q_t = 1/\beta \ln(\alpha\beta) + 1/\beta \ln(t) \quad (18)$$

Where q_t is the quantity of gas adsorbed during the time t (mg/g); α is the initial adsorption rate (mg/min); β is the extent of surface coverage and activated energy (g/mg); and t is the contact time (min). The Elovich constants, α and β at different temperatures were determined from the slope and intercept of the plot of q_t versus ln(t) as presented in Figures 37 and 38. The results of α and β were evaluated and listed in Tables 6 and 7. The values α for both dyes decreased with increase in temperature from 303K to 323K. This shows that as adsorption rate decreased, desorption rate increased with increased temperature. The values of the correlation coefficient R^2 ranged from 0.903 to 0.922 for orange G dye and 0.878 to 0.902 for safranin O dye as temperature of adsorption varied from 303K to 323K. This shows that the graphs conform to the model. However, similar results were obtained by Oladoja *et al*. (2008).

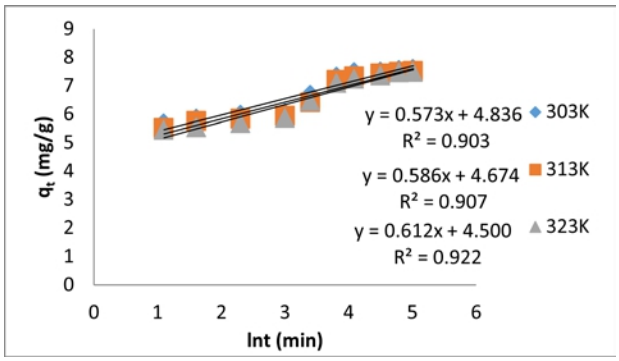

Fig 37: Elovich model kinetic plot for orange G dye on acid activated tamarind seed carbon.

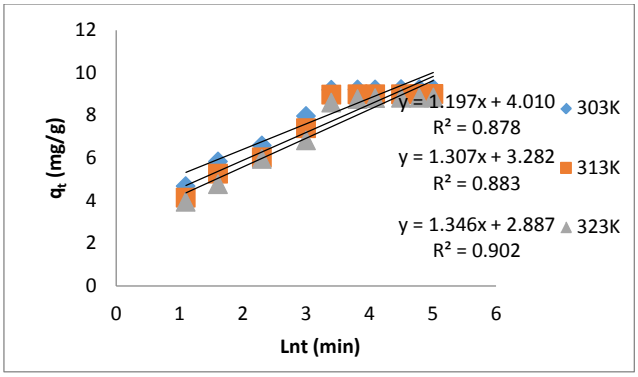

Fig 38: Elovich model kinetic plot for safranin O dye on acid activated tamarind seed carbon.

The Bhattacharya-Venkobachar model (Goswami and Ghosh, 2005) is expressed as:

$$\ln(1 - U_t) = K_B t \qquad (19)$$

$$U_t = {C_o - C_t}/{C_o - C_e} \qquad (20)$$

Effective diffusion Coefficient D_2 is obtained from the equation;

$$D_2 = {K_B r^2}/{\pi^2} \qquad (21)$$

Where r is the particle radius (m); K_B is the Bhattacharya-Venkobachar rate constant; C_o is the initial concentration (mg/L); C_e is the equilibrium concentration (mg/L); C_t is the equilibrium concentration at time, t (mg/L); U_t is the Bhattacharya-Venkobachar constant; and t is contact time (min).

The Bhattacharya-Venkobachar rate constants, K_B for all adsorbents at different temperatures were determined from the slope of the plot of ln(1-U_t) versus t as presented in figures 39 and 40. The results of K_B and D_2 were evaluated and listed in Tables 6 and 7. The correlation coefficient values R^2 ranged from 0.954 to 0.976 for orange G dye and 0.866 to 0.937 for safranin O dye, as temperature of adsorption varied from 303K to 323K. Thus, this indicates that the kinetic data followed Bhattacharya-Venkobachar model.

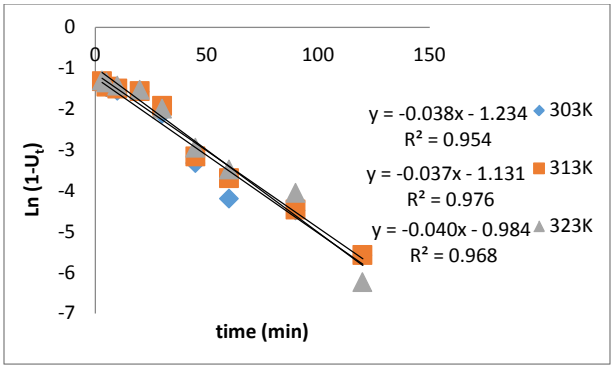

Fig 39: Bhattacharya-Venkobachar kinetic model plot for orange G dye on acid activated tamarind seed carbon.

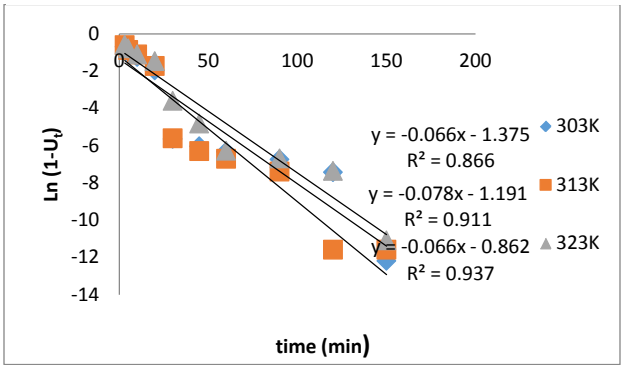

Fig 40: Bhattacharya-Venkobachar kinetic model plot for safranin O dye on acid activated tamarind seed carbon.

Intra Particle Diffusion Kinetic Model

The intra-particle diffusion equation is expressed as (Weber et al., 1972):

$$q_t = Kt^{0.5} + C_t \qquad (22)$$

Where q_t is the amount of dye adsorbed at time t (mg/g); K is the rate constant of the intra particle transport (g/mg/min); C_t is the equilibrium concentration (mg/L); and t is the contact time (min). The intra-particle diffusion rate constants, K and C_t at different temperatures were determined from the slope and intercept of the plot of q_t versus $t^{0.5}$ as presented in Figures 41 and 42. The results of K and C_t were evaluated and listed in Tables 6 and 7. The values of the correlation coefficient R^2 ranged from 0.926 to 0.948 for orange G dye, and 0.943 to 0.961 for safranin O dye, as temperature of adsorption varied from 303K to 323K. The high correlation coefficients for both dyes indicate the presence of intra-particle diffusion as the rate determining step. The rate limiting step that is the slowest step of the

reaction may be the intra-particle diffusion or the boundary layer of solute on the solid surface from the bulk of the solution in a batch process (Goswani and Ghosh, 2005). As shown in Figures 41 and 42, the linear lines did not pass through the origin due to the difference in mass transfer rate from the initial to the final stage of adsorption. The deviation of the linear lines from the origin indicates that intra-particle transport is not the sole rate limiting step, but other kinetic models may control the rate of adsorption simultaneously (Abechi *et al.*, 2011).

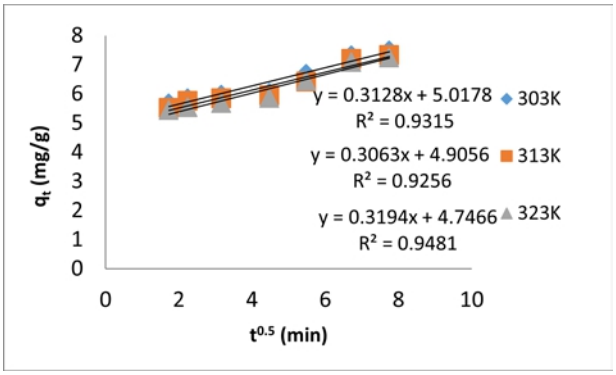

Fig 41: Intra particle diffusion kinetic model plot for orange G dye on acid activated tamarind seed carbon.

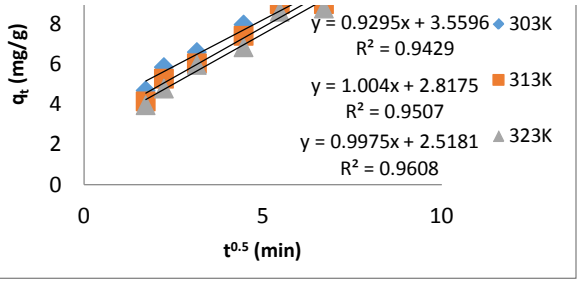

Fig 42: Intra particle diffusion kinetic model plot for safranine o dye on acid activated tamarind seed carbon.

TABLE 6: Kinetics Studies for Acid Activated Tamarind Seed Using Orange G Dye

Models	**Parameters**	**303K**	**313K**	**323K**
Pseudo-first order	K_1 (min^{-1})	-0.038	-0.047	-0.043
q_e (mg/g)	2.214	3.190	3.174	
R^2	0.954	0.940	0.972	
Pseudo-second order	K_2 (g/mgmin)	0.045	0.039	0.038
q_e (mg/g)	7.752	7.692	7.634	
R^2	0.999	0.999	0.999	
Elovich	α (mg/gmin)	2651.607	1705.603	955.198
β (g/mg)	1.745	1.706	1.634	
R^2	0.903	0.907	0.922	
Intra particle diffusion	K (g/mg/min)	0.313	0.306	0.319
C_t (mg/L)	5.018	4.906	4.747	
R^2	0.932	0.926	0.948	
Bhattacharya-Venkobachor	K_B	-0.038	-0.037	-0.040
D_2 (m^2/g)	-2.17×10^{-11}	-2.11×10^{-11}	-2.28×10^{-11}	
R^2	0.954	0.976	0.968	

TABLE 7: Kinetics Studies for Acid Activated Tamarind Seed Using Safranine O Dye

Models	**Parameters**	**303K**	**313K**	**323K**
Pseudo-first order	K_1 (min^{-1})	-0.048	-0.078	-0.051
	q_e (mg/g)	1.461	2.724	2.578
	R^2	0.763	0.91	0.872
Pseudo-second order	K_2 (min^{-1})	0.040	0.032	0.027
	q_e (mg/g)	9.434	9.346	9.179
	R^2	0.999	0.999	0.999
Elovich	α (mg/gmin)	34.119	16.100	11.496
	β (g/mg)	0.835	0.765	0.743
	R^2	0.878	0.883	0.902
Intra particle diffusion	K (g/mg/min)	0.930	1.004	0.998
	C_t (mg/L)	3.560	2.818	2.518
	R^2	0.943	0.951	0.961
Bhattacharya-Venkobachor	K_B	-0.066	-0.078	-0.066
	D_2 (m^2/g)	-3.76×10^{-11}	-4.44×10^{-11}	-3.76×10^{-11}
	R^2	0.866	0.911	0.937

Thermodynamics Study

The aim of thermodynamic study is to determine the spontaneity of the adsorption process by the use of thermodynamic parameters such as free energy change (ΔG^0), enthalpy change (ΔH^0), and entropy change (ΔS^0). ΔG^0 determines if the process is feasible and spontaneous or not; ΔH^0 determines if the process is exothermic or endothermic; and ΔS^0 determines the increase or decrease in randomness of the process at the solid/solution interface. Reactions occur spontaneously at a given temperature if ΔG^0 is a negative quantity (Abdessalem *et al.*, 2012). The temperatures used in the thermodynamic study were 303K, 313K, and 323K. The thermodynamic parameters were calculated based on the following equations:

$$\Delta G^{\circ} = -RT \ln(K) \quad (23)$$

$$\Delta G^{\circ} = \Delta H^{\circ} - T\Delta S^{\circ} \quad (24)$$

Where T is the absolute temperature (K), R is the universal gas constant (8.314J/mol/K) and K is the Langmuir constant. The Gibbs free energy of adsorption (ΔG^0) can be related with the equilibrium constant K (L/mol), corresponding to the reciprocal of the Langmuir constant b (Oladoja *et al*, 2008). The values of the thermodynamic parameters using orange G and safranin O dye are listed in Table 8. The negative ΔG^0 values indicate that the process is thermodynamically feasible and spontaneous. The negative ΔH^0 values indicate that the nature of adsorption process is exothermic. This is also supported by the decrease in the value of adsorbed capacity of the sorbent with the increase in temperature. The positive values of ΔS^0 pointed to an increased disorder of the solid/solution interface during the adsorption process. However, similar results were obtained by Gunasekar and Ponnusami (2012).

Table 8: Thermodynamics Studies for Acid Activated Tamarind Seed

Dyes	T(K)	ΔG (KJ/mol)	ΔS (J/mol K)	ΔH (KJ/mol)
Orange G	303	-22.39		
313	-22.96	0.046	-8.488	
323	-23.31			
Safranin O	303	-22.77		
313	-22.47	0.007	-24.87	
323	-22.63			

Conclusion

Adsorption process has been successfully used in the dye-based wastewater treatment using activated carbons obtained from tamarind seeds. The proximate analysis carried out on the activated carbon show that each property value was in good range. The Fourier transform infrared spectroscopic analysis done on the non-acid activated adsorbent and acid activated adsorbent shows the presence of functional groups (alkanes, alkenes, alkynes, carboxyl, phenols, etc.) which are very important adsorption sites. The X-ray Diffraction analysis shows the presence of high diffraction peaks and broadness which are evidence of good crystallinity of the prepared powdered samples. The Scanning Electron Microscopy images show various shape and pore sizes at different magnifications. The batch adsorptive studies carried out shows that particle size, pH, adsorbent dosage, ion concentration, and contact time are effective on the adsorption of dyes from wastewater using tamarind seed adsorbents. The Freundlich isotherm model best fitted the equilibrium data obtained. Pseudo-Second order kinetic model best describes the adsorption kinetics carried out. Thus, the thermodynamic parameters calculated which shows that the adsorption

process is feasible, has an increased disorder of solid-solute interface, and is also exothermic in nature.

References:

Abdessalem, O., Ahmed, W., Mourad, B. Adsorption of Bentazon on Activated Carbon Prepared from Lawsonia Inermis Wood. Equilibrium and Thermodynamic studies, Arabian Journal of Chemistry. 10, 1016, 2012.

Abechi, E. S., Gimba, C. E., Uzairu, A., Kagbu, J. A. Kinetics of Adsorption of Methylene Blue onto Activated Carbon Prepared from Palm Kernel Shell. Arch. Appl. Sci. Res. 3(1), 154-164, 2011.

Aharoni, C. and Sparks, D. L. 'Kinetics of Soil Chemical Reaction-A Theoretical Treatment' in D. L.

Sparks and D. L. Suarez (eds), Rates of soil chemical processes, soil science society of America, Madison, Wi, pp. 1-18, 1991.

American Society for Testing and Materials: Standard for Method for Determination of Iodine Number of Activated Carbon. Philadelphia, PA: ASTM Committee on Standards, 1986.

American Society for Testing and Materials: Standard for Method for Moisture in Activated Carbon. Philadelphia, PA: ASTM Committee on Standards, 1991.

American Society for Testing and Materials: Standard Method for the Determination of pH value in Biomass, Philadelphia, P.A.: 11, (05), 1996.

American Society for Testing and Materials: Standard Method for the Determination of Ash in Biomass, Philadelphia, P.A.: 11, (05), 2003.

Andre, L. C., Alexandro, M. M., Eurica, M. N., Marcos, H. K., Marcos, R. G., Alessandro, C. N., Tais, L. S., Juliana, C. G., and Victor, C. A. NaOH-Activated Carbon of High Surface Area Produced from Coconut Shell: Kinetics and Equilibrium Studies from the Methylene Blue Adsorption. Chemical Engineering Journal, 174: 117-125, 2011.

Banat F., Al-Asheh S., Masad A. Physical and Chemical Activation of Purolyzed Oil Shade Residue for the Adsorption of Phenol from Aqueous Solution. Environmental Geology 44: 333-342, 2003.

Bulut, Y. and Aydin, H. A Kinetic and Thermodynamics Study of Methylene Blue Adsorption on Wheat Shells. Desalination, 194: 259-267, 2005.

Cheremisinoff, N. P. and Chermisinoff, P.N. Carbon Adsorption for Pollution Control; Prentice Hall, Englewood Cliffs, NJ, 1993.

Dada, A. O., Olalekan, A. P., Olatunya, A. M. Isotherm Studies of Equilibrium Sorption of Zn^{2+} Unto Phosphoric Acid Modified Rice Husk. IOSR Journal of Applied Chemistry, ISSN: 2278-5736, 3: 38-45, 2012.

El-Hendawy, A. A., Alexander, R. J., Andrews, G. F. Effect of Activation Schemes on Porous Surface and Thermal Properties of Activated Carbins Prepared from Cotton Stalk, J. Anal. Appl. Pyrolysis, 82: 272-278, 2008.

Garg, V. K., Moirangthem Amita, Rakesh Kumar, Renuky Gupta. Basic Dye Removal from Simulated Wastewater by Adsorption Using Rose Wood Sawdust: A Timber Industry Waste, Dyes and Pigments. 63: 243-250, 2004.
Goswami, S., and Ghosh, U. C. Studies on Adsorption Behaviour of Cr(VI) onto Synthetic Hydrous Stannic Oxide. Water S A, 31 (4), 597-602, 2005.
Gregg, S. J. and Sing, K. S. W. Adsorption Surface Area and Porosity. Academic Press, 1982.
Gunasekar, V. and Ponnusami, V. Kinetics, Equilibrium, and Thermodynamic Studies on Adsorption of Methylene Blue by Carbonized Plant Leaf Powder. Journal of Chemistry, Volume 2013 (2013), Article ID 415280, 6pages.
Gurses, A., Dogar, C., Yalc-in, M., Acikyildiz, M., Bayrak, R. The Adsorption Kinetics of Cationic Dye Methylene Blue onto Clay. J. of Haz. Mat. 131: 217-228, 2006.
Haimour, N. M. and Emeish, S.Utilization of Date Stones for Production of Activated Carbon using Phosphoric Acid. Waste Manage, 26, 651– 660, 2006.
Hasany, S. M. and Chaudhary, M. H. 'Sorption Potential of Hare River Sand for the removal of Antimony from Acidic Aqueous Solution; Appl. Rad. Isotopes 47: 467-471, 1996.
Ho, Y. S., Chiang, C. C. Sorption Studies of Acid Dye by Mixed Sorbents. Adsorption 7: 139-147, 2001.
Ho, Y.S., Mckay, G. Sorption of Dye from Aqueous Solution by Peat, Chem. Eng. J. 70(2), 115-124, 1998.
Horsfall, M., Spiff, A. I., Abia, A. A. Studies on the Influence of Mercaptoacetic Acid Modification of Cassava Waste Biomass on the Adsorption of Cu^{2+} and Cd^{2+} from Aqueous Solution. Bull. Korean Chem. Soc., 25(7), 969-976, 2004.
Joseph. T. N. and Philomena, K. I. Copper (II) Uptake by Adsorption Using Palmyra Palm Nut. Adv. Appl. Sci. Res. 2(6), 166-175, 2011.
Juang, R. S., Wu. F. C., Tseng, R. L. Ability of Activated Clay for the Adsorption of Dyes from Aqueous Solution: Environ. Technol., 18: 535, 1997.
Kesari, K. K., Verma, H. N., Behari, J. Physical Methods in Wastewater Treatment: Sono Chemistry: Environmental Science and Engineering Application in Wastewater, LAP LAMBERT Academic Publishing, 152, 2011.
Khan, T. A., Ali, I., Singh, V. V., Sharma, S. Utilization of Fly Ash as Low Cost Adsorbent for the Removal of Methylene Blue, Malachite Green, and Rhodamine B Dyes from Textile Waste Water. Journal of Environmental Protection Science, 3: 11-22, 2009.

Klaus Christmann. Modern Methods in Heterogenous Catalysis Research. Lecture Series Institute for Chem. and Biochem. Uni. Berlin, 2010.
Lagergren, S. About the Theory of So-called Adsorption of Soluble Substance. Kunliga Svenska Velenskap-Sakademiens. Handlingar, 24(4), 1-39, 1898.
Okiemmen, F., Okiemen, C., Wuana, A. Preparation and Characterization of Activated Carbon from Rice Husk. Journal of Chemical Society of Nigeria, 32, 126-136, 2008.
Oladoja, N. A., Aboluwoye, C. O., Oladimeji, Y. B. Kinetics and Isotherm Studies on Methylene Blue Adsorption onto Ground Palm Kernel Coat. Turkish J. Eng. Env. Sci., 32: 303-312, 2008.
Ozacar, M. and Sengil, A. I. Adsorption of Reactive Dyes on Calcined Alunite from Aqueous Solutions. J. Hazard Matter. 98: 211-224, 2003.
Rahman, M. A., Amin, A. R. R., Alam, S. A. M. Removal of Methylene Blue from Waste Water Using Activated Carbon Prepared from Rice Husk, Dhaka Univ. J. Sc. 60(2), 185- 189, 2012.
Sekar, M., Sakthi, V., & Rengaraj, S. Kinetics and Equilibrium Adsorption Study of Lead (II) Onto Activated Carbon Prepared from Coconut Shell: Journal of Colloid and Interface Science, 279(2), 307-313, 2004.
Singh, J., Mishra, N. S., Sushmita, B. Comparative Studies of Physical Characteristics of Raw and Modified Sawdust for their Use as Adsorbents for Removal of Acid Dye: BioResouirces 6(3): 2732-2743, 2011.
Suresh Jeyakumar. SEM, FTIR and XRD Studies for the Removal of Cu(II) from Aqueous Solution Using Marine Green Algae. J. Global Research Analysis 2(11): 2277-8160, 2013.
Verla, A. W., Horsfall M., Veria, E. N., Spiff, A. N., Ekpete, O. A. Preparation and Characterization of Activated Carbon from Fluted Pumpkin Seed Shell. ASIAN Journal of Natural and Applied Sciences. 1(3), 2012
Wang, C. C., Juang, L. C., Hsu, T. C., Lee, C. K., Lee, J. F., Huang, F. C. Adsorption of Basic Dyes onto Montmorillionite Colloid. Int. Sci. 272: 80-86, 2004.
Weber, W. J., Jr. Physicochemical Processes: for Water Quality Control: Wiley-Interscience, John Wiley and Sons. New york, 199-259, 1972.